Remote Sensing of Environment 211 (2018) 218–228

Contents lists available at ScienceDirect

Remote Sensing of Environment

journal homepage: www.elsevier.com/locate/rse

Influence of species richness, evenness, and composition on optical diversity: A simulation study

Ran Wang[a,*], John A. Gamon[a,b,c], Anna K. Schweiger[d], Jeannine Cavender-Bares[d], Philip A. Townsend[e], Arthur I. Zygielbaum[c], Shan Kothari[f]

[a] Department of Earth and Atmospheric Sciences, University of Alberta, Edmonton, AB T6G 2E3, Canada
[b] Department of Biological Sciences, University of Alberta, Edmonton, AB T6G 2E9, Canada
[c] School of Natural Resources, University of Nebraska-Lincoln, Lincoln, NE 68583, USA
[d] Department of Ecology, Evolution and Behavior, University of Minnesota, Saint Paul, MN 55108, USA
[e] Department of Forest and Wildlife Ecology, University of Wisconsin-Madison, Madison, WI 53706, USA
[f] Department of Plant Biological Sciences, University of Minnesota, Saint Paul, MN 55108, USA

ARTICLE INFO

Keywords:
Biodiversity
Remote sensing
Optical diversity
Imaging spectroscopy
Cedar Creek

ABSTRACT

While remote sensing has increasingly been applied to estimate α biodiversity directly through optical diversity, there is a need to better understand the mechanisms behind the optical diversity-biodiversity relationship. Here, we examined the relative contributions of species richness, evenness, and composition to the spectral reflectance, and consider factors confounding the remote estimation of species diversity in a prairie ecosystem experiment at Cedar Creek Ecosystem Science Reserve, Minnesota. We collected hyperspectral reflectance of 16 prairie species using a tram-mounted imaging spectrometer, and a full-range field spectrometer with a leaf clip, and simulated plot-level images from both instruments with different species richness, evenness and composition. Two optical diversity metrics were explored: the coefficient of variation (CV) of spectral reflectance in space and classified species derived from Partial Least Squares Discriminant Analysis (PLS-DA), a spectral classification method. Both optical diversity metrics (CV and PLS-DA classified species) were affected by species richness and evenness. Diversity metrics that combined species richness and evenness together (e.g. Shannon's index) were more strongly correlated with optical diversity than either metric alone. Image-derived data were influenced by both leaf traits and canopy structure and showed larger spectral variability than leaf clip data, indicating that sampling methods influence optical diversity. Leaf and canopy traits both contributed to optical diversity, sometimes in complex or contradictory ways. Large within-species variation sometimes confounded biodiversity estimation from optical diversity, and a single species markedly altered the optical-biodiversity relationship. Biodiversity estimation from CV was strongly influenced by soil background, while estimation from PLS-DA classified species was not sensitive to soil background. These findings are consistent with recent empirical studies and demonstrate that modeling approaches can be used to explore effects of spatial scale and guide regional studies of biodiversity estimation using high spatial and spectral resolution remote sensing.

1. Introduction

"Optical diversity" (Ustin and Gamon, 2010), sometimes called "spectral diversity" (Palmer et al., 2002), indicates the variation in spectral reflectance detected by optical remote sensing. Many remote sensing indices have been applied to assess vegetation diversity and composition using optical measurements. These metrics can be divided into two major categories: 1) species-based metrics; and 2) information content-based metrics. Species-based metrics typically apply a classification, either unsupervised (Féret and Asner, 2014) or object-based (Schäfer et al., 2016), to the remotely sensed images. Indices calculated using these classified "spectral species" (Féret and Asner, 2014) are then related to plant diversity. Here, we expanded the term "spectral species" (Féret and Asner, 2014) to species classified from remote sensing data using any classification method. In this case, spectral species are considered proxies for biological species, and spatial variation in spectral species can be used to infer species richness or other metrics of α diversity, and over larger areas, β diversity.

Several factors conspire to complicate species-based methods of detecting biodiversity using remote sensing. Variation of plant leaf

* Corresponding author.
E-mail address: rw6@ualberta.ca (R. Wang).

https://doi.org/10.1016/j.rse.2018.04.010
Received 16 September 2017; Received in revised form 23 March 2018; Accepted 5 April 2018
Available online 24 April 2018
0034-4257/

traits and canopy structure across environmental gradients (i.e. phenotypic variation) can lead to high spectral variability within species (Asner, 1998). Similarly, temporal variation in leaf traits, e.g., due to leaf aging, can generate large intra- and interspecific variation, which could potentially confound species identification through spectral reflectance (Chavana-Bryant et al., 2017). These challenges in species-based approaches to biodiversity detection have led to alternate methods based on information content.

Information content-based metrics extract information from the spectral space in a number of ways, for example, by calculating the variance of vegetation reflectance indices (e.g., NDVI) (Carlson et al., 2007; Gould, 2000), the coefficient of variation derived from spectral reflectance (Wang et al., 2016a), or the distance from the spectral centroid (Palmer et al., 2002). Alternatively, information content-based metrics can be obtained from patterns in principal component space, such as the distance from the centroid (Rocchini, 2007), which compacts spectral information and removes noise and band collinearity (Thompson et al., 2017).

When comparing optical diversity to α diversity, stronger relationships emerge when considering both species richness and evenness (e.g., Shannon's index) relative to either diversity measure alone (Oldeland et al., 2010; Wang et al., 2016a). Species evenness adds additional information on stand composition, which affects spectral variation. However, it is not clear how or to what extent species richness, evenness, and composition affect the overall optical signal, in part because experimental approaches are difficult to apply in remote sensing studies due to the large spatial scales involved. Furthermore, soil is known to confound optical diversity estimation (Gholizadeh et al., 2018) and these effects (species richness, evenness, composition and soil background) can be scale-dependent (Wang et al., 2018) requiring studies to be explicit about the spatial, temporal and spectral scales involved.

To help address these issues, we applied a modeling framework to investigate the effect of species richness, evenness and composition on optical diversity using simulated hyperspectral images. For this simulation, leaf reflectance measurements collected in the Cedar Creek long-term biodiversity experiment (BioDIV) (Reich et al., 2012; Tilman, 1997) were used to model synthetic plot-level images with different combinations of species richness, evenness, and composition. In this modeling study, leaf spectra were collected in two ways: 1) using a leaf clip that normalized sampling geometry and illumination; and 2) using an imaging spectrometer mounted on a tram system that allowed for natural variation in leaf orientation and illumination. Two types of optical diversity metrics, the coefficient of variation (CV) and spectral species derived from Partial Least Squares Discriminant Analysis (PLS-DA) (Peerbhay et al., 2013), were used to estimate vegetation diversity. In this study, by calculating optical diversity metrics on simulated images derived from leaf-level and image-derived spectra, we addressed the following four questions: 1) how do species richness, evenness, and composition affect optical diversity? 2) how do sampling methods affect optical diversity? 3) how does within-species variation affect the optical diversity-vegetation diversity relationship? and 4) how does soil background affect optical diversity?

2. Methods

2.1. Study site

Data used in this study were collected at the Cedar Creek Ecosystem Science Reserve, Minnesota, USA (45.40° N, 93.19° W). Since 1994, the BioDIV experiment has maintained 167 experimental plots (9 m × 9 m) with planted species richness ranging from 1 to 16 species per plot (Tilman, 1997). The species planted in each plot were randomly selected from a pool of 18 species typical of Midwestern prairie, including C_3 and C_4 grasses, legumes, forbs and trees. Plots were weeded 3 to 4 times each year to remove species not included in the desired pool (Reich et al., 2012; Tilman et al., 2001).

Table 1
Species, abbreviations, and sample size per species of leaf reflectance spectra.

Species	Abbrev	No. of samples
Achillea millefolium L.	ACHMI	134
Amorpha canescens Pursh	AMOCA	88
Andropogon gerardii Vitman	ANDGE	577
Asclepias tuberosa L.	ASCTU	249
Koeleria cristata auct. non Pers. p.p.	KOECR	44
Lespedeza capitata Michx.	LESCA	370
Liatris aspera Michx.	LIAAS	195
Lupinus perennis L.	LUPPE	380
Monarda fistulosa L.	MONFI	74
Panicum virgatum L.	PANVI	169
Petalostemum candidum (*Willd.*) *Michx.*	PETCA	88
Petalostemum purpureum (*Vent.*) *Rydb.*	PETPU	157
Petalostemum villosum Nutt.	PETVI	137
Poa pratensis L.	POAPR	49
Schizachyrium scoparium (Michx.) Nash	SCHSC	260
Solidago rigida L.	SOLRI	173

2.2. Spectral data

2.2.1. Leaf-level reflectance

We collected leaf level reflectance using a full range spectrometer (HR-1024i, Spectral Vista Corporation, Poughkeepsie, NY, USA) coupled with a leaf clip with an internal light source (LC-RP PRO; Spectra Vista Corporation, Poughkeepsie, NY, USA). The spectral range of the spectrometer covered 340.5 to 2522.8 nm in 1024 spectral bands. Noisy spectral regions (wavelengths smaller than 400 nm and > 2400 nm) were excluded from analysis. During field measurements, leaf level measurements ($L_{target,\lambda}$) were referenced to a white calibration disc of the leaf clip ($L_{white\ reference,\lambda}$) approximately every 5 min. Dark current radiance was subtracted internally, and relative spectral reflectance was calculated as (ρ_λ):

$$\rho_\lambda = L_{target,\lambda}/L_{white\ reference,\lambda} \quad (1)$$

We measured up to 16 prairie species (Table 1) in 24 BioDIV plots. We visually divided each plot into 9 subplots and sampled four, six or eight subplots, depending on the planted species richness (four for one or two planted species per plot, six for four species per plot, and eight for eight or 16 species per plot). We randomly placed a 1 × 1 m frame in each sampled subplot and measured one individual of each of the four most abundant species, with duplication of species possible when we found fewer than four species per subplot. As a consequence, the sample size of each species correlated with the abundance of that species encountered during our field sampling.

In order to measure reflectance of grasses and herbaceous species with small leaves, we aligned small leaves in the foreoptic, avoiding overlap of adjacent leaves, covering a minimum of about 50% of the field of view. We judged a measurement as “good” when reflectance in the NIR shoulder (about 800 nm) was as at least 35% or higher. Soil radiance spectra were collected using a full range spectrometer (PSR 3500, Spectral Evolution, Lawrence, MA, USA) coupled with a 4-degree lens (Spectral Evolution, Lawrence, MA, USA) in the bare ground plots of the BioDIV experiment in July 2016. A white reference panel (Spectralon, Labsphere, North Sutton, NH, USA) was used to calculate relative reflectance of the soil. The leaf-level data is available from EcoSIS Spectral Library (https://data.ecosis.org/dataset/leaf-spectra-big-biodiversity-experiment-cedar-creek-lter).

2.2.2. Image-derived reflectance

A push-broom imaging spectrometer (E Series, Headwall Photonics Inc., Fitchburg, MA, USA) mounted on a tram system (Gamon et al., 2006) at 3 m above the ground surface was used to collect fine-scale images (1 mm^2 pixel resolution) of the northern-most row of each

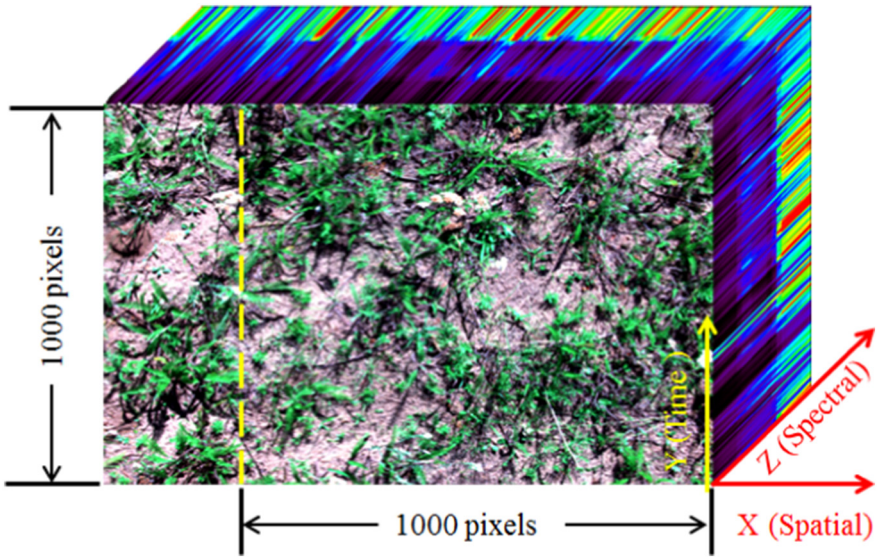

Fig. 1. Sample image cube from Plot 11, richness = 1 (*Achillea millefolium*) obtained by the Headwall imaging spectrometer showing spatial and spectral dimensions (red arrows, covering reflectance from 400 to 1000 nm). The yellow vector indicates the direction of cart motion. For each image, 600 1 × 1 mm pixels from the north side of each scan line (pixels to the left of the yellow dashed line) were removed from the original image to minimize edge effects, leaving a square image cube (1000 × 1000 pixel) for further analysis. (For interpretation of the references to color in this figure legend, the reader is referred to the web version of this article.)

sampling plot at the peak of growing season in 2015 (July 17 to July 26, 2015) (Wang et al., 2018). The same 16 species measured with the SVC field spectrometer were identified from the hyperspectral images (Fig. 1) and a sample of 1000 leaf pixels of each species was selected to create a pool of image-derived reflectance spectra. Unlike leaf clip-derived measurements, where leaf spectra were collected under normalized geometry and illumination, image-derived spectra provided a large sample of leaves in their natural orientation and illumination, collectively comprising a "canopy" spectrum for each species. This set of image-derived spectra allowed us to explore the effect of including natural variation in leaf reflectance due to illumination and plant geometry (e.g., leaf area index and leaf angle distribution) for comparison with leaf clip-derived spectra where such variation was minimized. Soil reflectance spectra were extracted from the bare-ground images of low richness plots. All hyperspectral images are available from NASA LPDAAC (doi: https://doi.org/10.5067/Community/Headwall/HWHYPCCMN1MM.001).

2.3. Spectral variability among/within species

We applied a nonparametric multivariate analysis of variance (NPMANOVA) to test whether species can be separated spectrally using Euclidean distances among species' spectra. NPMANOVA was first developed for tests of differences among ecological groups (Anderson, 2001). A pseudo *F*-statistic is calculated as the ratio between sum of squares among-species and sum of squares within-species (Anderson, 2001), with a large *F* value falsifying the null hypothesis (H_0: no difference among species). The significance of the *F* value was tested against a null distribution of *F* based on random permutations (Anderson, 2001). The Euclidean distance (*d*) between two spectra (S_1 and S_2), is the root mean square difference between them, averaged over the whole spectral range:

$$d = \left[\frac{1}{N} \sum_{i=1}^{N} [S_1(\lambda_i) - S_2(\lambda_i)]^2 \right]^{1/2} \quad (2)$$

We also applied a PLS-DA classification method to test the separability of different species. PLS-DA has been gaining attention for its ability to accommodate high-dimensional classification problems by handling high collinearity among predictors (Chung and Keles, 2010; Nguyen and Rocke, 2002) and has been used to classify tree species using airborne remote sensing (Peerbhay et al., 2013). In this study, the PLS-DA classification was calculated using the caret R package (Kuhn, 2008). Each dataset was randomly split into two-thirds for training and one-third for testing. The training set was used to optimize the classification model, while the testing set was used to validate the optimized classification model. We also used the mean reflectance of each species to test the classification model. The overall accuracy and unweighted Kappa statistic were calculated based on the confusion matrix for the actual and predicted species identities.

2.4. Generation of plot-level synthetic images

To investigate the individual effects of species richness, evenness, and composition on spectral diversity, we simulated 1000 synthetic plots consisting of 10,000 spectra per plot as follows: 1) we randomly assigned a species richness level (between 1 and 16) to each plot; 2) we calculated the total vegetation cover of each plot according to the estimated species richness-percent cover relationship (Supplemental section 1); 3) we then randomly generated the percent cover of each species (the range of percent cover for each species varies from 1% to 100%, with the total vegetation percentage cover of all the species present smaller than 100%); and 4) finally, we filled the remainder of the image with soil spectra.

To help decipher the effects of within- vs. among-species variability on optical diversity, we used two methods of generating synthetic images for each plot: one used the mean reflectance of each species, which ignored within-species variation in spectral reflectance, and the other used all reflectance spectra per species including variation due to leaf traits and canopy structure. Both leaf level and image-derived spectra were used to generate synthetic images, resulting in four sets of simulated images per plot (leaf level mean reflectance of each species, leaf level all reflectance, image-derived mean reflectance of each species, image-derived all reflectance).

2.5. Optical diversity and conventional vegetation diversity metrics

For each simulated plot-level image we calculated two categories of optical diversity metrics: a) the coefficient of variation (CV), which relates to the information content or spectral "complexity" of each plot (Rocchini et al., 2010; Wang et al., 2016a), and b) three indices based on spectral species obtained from PLS-DA classification: spectral species richness, and two abundance weighted metrics, including the spectral species Shannon's index (Shannon, 1948), and spectral species Simpson's index (Simpson, 1949; Williams, 1964).

The average CV for each wavelength was used as an indicator of spectral diversity:

Table 2
Summary of vegetation diversity metrics used in this study.

Diversity metric	Description/equation
Species richness (*S*)	Number of species
Shannon's index (*H′*) (Shannon, 1948)	$H' = -\Sigma p_i * \ln(p_i)$
The reciprocal of Simpson's index (*D*) (Simpson, 1949; Williams, 1964)	$D = 1/\sum p_i^2$
Evenness (*J′*) (Pielou, 1966)	$J' = H'/\ln(S)$

Where p_i is percent cover proportion of the number i^{th} species.

$$CV = \frac{\sum_{\lambda 1}^{\lambda 2}\left(\frac{\sigma(\rho_\lambda)}{\mu(\rho_\lambda)}\right)}{N} \quad (3)$$

where $\sigma(\rho_\lambda)$ and $\mu(\rho_\lambda)$ indicate the standard deviation and mean value of reflectance at wavelength λ across all the pixels in one plot, respectively and *N* is the number of wavelengths. In this case, CV expresses the spectral heterogeneity among pixels with one single value per plot. For leaf-level data, we calculated CV for VIS-NIR region (400–1000 nm) and full spectral range (400–2500 nm) separately to investigate the effects of spectral range on optical diversity-vegetation diversity relationship. For image-derived data, we calculated CV using wavelengths from 430 nm to 925 nm, the range available from the imaging spectrometer.

Conventional vegetation diversity metrics (species richness and three abundance-weighted vegetation diversity indices (Table 2)) were calculated based on the vegetation percentage cover of each species and related to the optical diversity metrics (CV and spectral species based indices) of each simulated plot.

The research questions and experimental variables used to address these questions with the simulation approach are summarized in Table 3.

3. Results

3.1. Reflectance and spectral separability

The two sampling methods (leaf-level vs. image-derived spectra) led to clear differences in spectral variability, with implications for subsequent analyses. Leaf-level reflectance (i.e., leaf-clip-derived spectra) of the 16-prairie species showed properties typical of vegetation spectra (Roberts et al., 2004; Ustin et al., 2009): absorption of blue and red light by chlorophyll and other pigments, high reflectance in the near infrared due to the multiple scattering, weak NIR water absorption features near 980 and 1200 nm, and strong water absorption near 1400 and 1900 nm (Fig. 2). Image-derived reflectance, covering the VIS-NIR region, showed patterns similar to the leaf clip-derived measurements in the visible region but had larger variation, particularly visible in the NIR region, resulting from varying plant geometry and illumination (Fig. 2).

The total variance of image-derived data was much larger than leaf clip-derived data (7.71 and 0.97, respectively). Patterns of within-species variation were different for leaf-level and image-derived reflectance (Figs. 3 and S2 in Supplemental material). For example, *Amorpha canescens* had the largest within-species variation for the leaf-level data, while *Petalostemum villosum* had the largest within-species distance for the image-derived data. The large within-species variation for *Petalostemum villosum* captured by image-derived reflectance reflected variation in individual canopy elements (leaves, stems and flowers) and canopy architecture.

Spectral separability of species can be successful if a large distance exists between different species in spectral feature space and if the within-species variation is less than among- species variation (Clark et al., 2005). In this study, among-species variability was greater than within-species variability for both leaf-level and image-derived measurements when using Euclidean distance as the spectral variability metric (as indicated by the large *F* values, Table 4). For leaf-level measurements, a slightly larger *F*-ratio was achieved when using full range spectra compared to VIS-NIR spectra, indicating that full range spectra increased species spectral separability, presumably by adding information on leaf structure, water, and biochemical content (Asner and Martin, 2009). The greater separation of species with image-derived spectra was presumably due to the added information of canopy structure and illumination; by contrast, standardized illumination and geometry of the leaf-level measurements removed spectral variation contributed by canopy structure and illumination. This result indicates that including variation in canopy structure, e.g. LAI, and leaf-angle distributions can increase species separability and that leaf traits alone do not fully explain optical diversity obtained from imaging techniques.

Table 3
Experimental tests and variables used for each test.

Experimental test	Experimental variables
Vegetation community composition	Species richness, evenness, and composition
Diversity indices	CV or spectral species (PLS-DA derived metrics)
Soil background	Soil vs. no soil
Spectral range	Full range (400–2400 nm) vs. VIS-NIR (400–1000 nm)
Within species variation	Full sample vs. mean spectra
Sampling methods (differences in plant geometry and illumination)	Leaf-level vs. image-derived spectra

3.2. Information content-based optical diversity (CV)

In accordance with larger spectral distance among species captured by image-derived reflectance relative to leaf-level reflectance, plot-level CV values calculated with image-derived reflectance had a larger range than CV values calculated with leaf-level reflectance (Fig. 4). However, leaf-level CV showed stronger relationships with vegetation diversity metrics than image-derived CV (Table 5). Using the mean reflectance spectrum of each species to simulate the plots resulted in the strongest relationships between plot-level CV and species richness for both leaf-level and image-derived data (Table 5). In addition, in all cases, linear relationships between the CV and diversity metrics that combined evenness with species richness (Shannon's index and Simpson's index) were stronger than the relationship between the CV and species richness alone, with the strongest relationship occurring between the CV and Shannon's index for leaf-level and image-derived spectra (Table 5).

For both sampling methods (leaf-level and image-derived), adding within-species variation by using the full set of spectra instead of the mean spectrum for each species increased the CV and weakened the relationships between the CV and all vegetation diversity metrics when no soil spectra were added (Table 5 and Fig. 4). For the image-derived reflectance, linear relationships between CV and diversity metrics almost disappeared (very small R^2) when all spectra were used instead of mean spectra. The statistically significant but weak relationships between optical diversity (CV) and vegetation diversity metrics presumably reflected the large sample (1000 synthetic plots) used in the regression.

Adding soil spectra to the simulation increased the plot level CV (Fig. 4), and greatly reduced the relationships with biodiversity metrics (S, H′, D, and J'). When using the mean reflectance of each species, including soil increased the plot level CV dramatically (approx. 500 times) and completely eliminated the CV-biodiversity relationships. When using the full set of spectral samples, adding soil also increased the CV and weakened the CV-biodiversity relationships, although most relationships remained significant. Image-derived CV was less sensitive to the inclusion of soil than the leaf-level CV (Table 5, Fig. 4). These results reveal that both the degree of cover and bare soil affected the

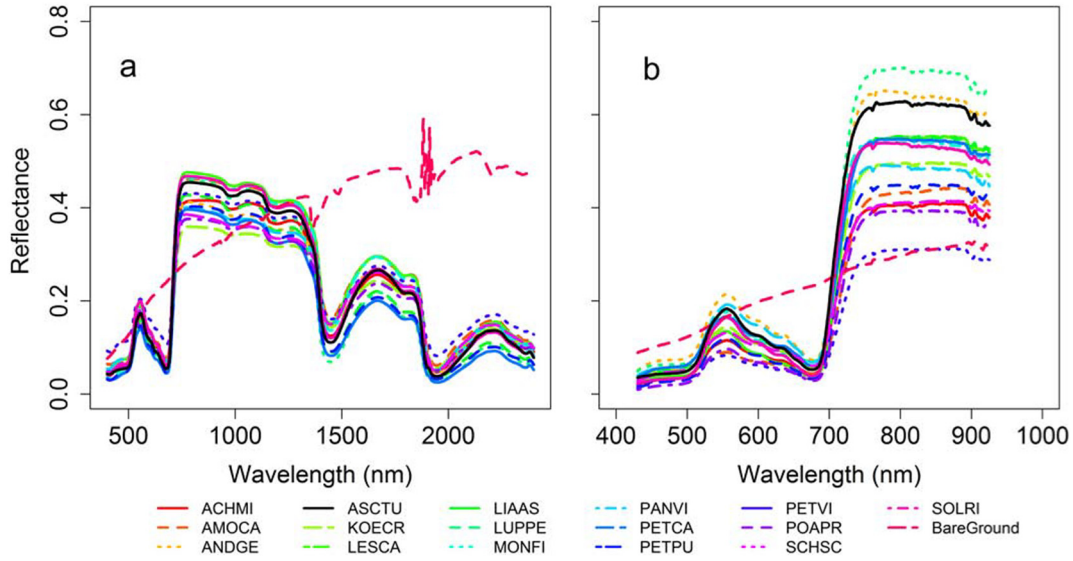

Fig. 2. Mean reflectance spectra of prairie species used in this study for (a) leaf-level reflectance obtained with a portable spectrometer and leaf clip covering 400–2400 nm; (b) image-derived leaf reflectance obtained with an imaging spectrometer mounted on a tram covering 400–1000 nm. Species abbreviations are given in Table 1.

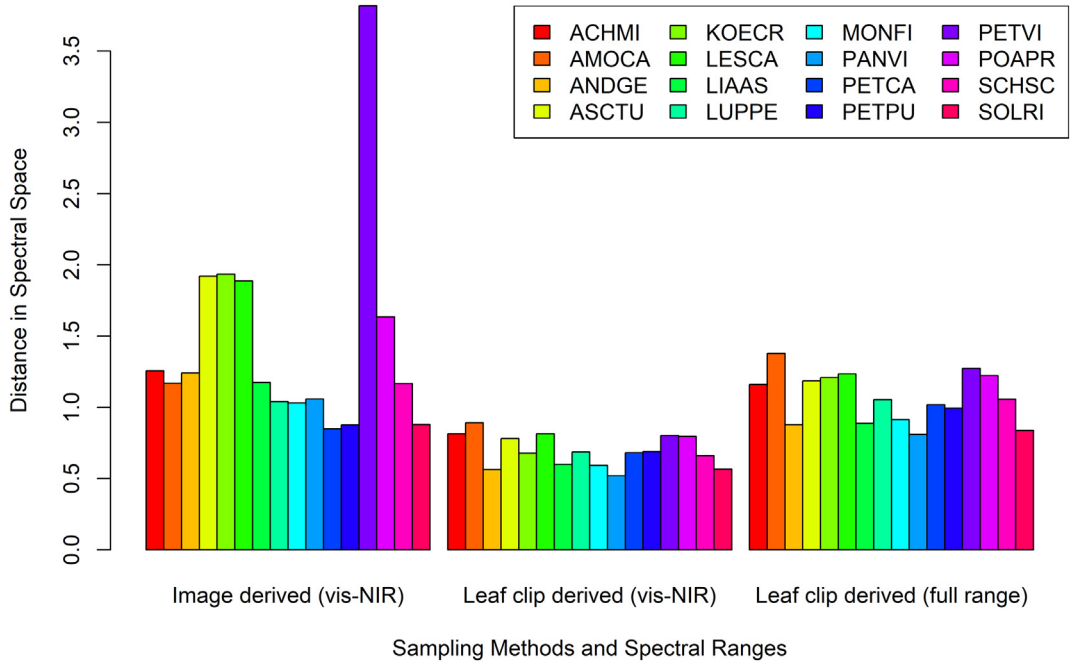

Fig. 3. Mean distance from centroid in spectral space of each species using two sampling methods (image-derived and leaf-clip-derived spectra) and two spectral ranges (visible-NIR and full-range). The clear outlier (high value) in the image-derived distance was *Petalostemum villosum* (PETVI), which was in flower during the measurements.

information content-based spectral diversity metrics, with bare soil lowering the ability to detect α diversity.

We analyzed the contributions of species richness and evenness to the plot-level CV and tested for possible interactions between species richness and evenness using ANOVA (Fig. 5 and Table 6). The shape of the CV-richness-evenness surfaces confirmed that both species richness and evenness affected the optical signal (Fig. 5). No statistically significant interaction between richness and evenness was found with leaf-level CV, while a weak interaction between richness and evenness was found with image-derived CV, indicating that the effect of species richness on the CV varied slightly with evenness (Table 6). For the image-derived reflectance, increasing richness and evenness generally increased CV values. However, it is important to note that a lot of large CV values were found at the low richness plots and the largest CV values occurred at one of the low richness plot (richness = 2), potentially confounding biodiversity detection.

3.3. Effects of species composition on CV

The large variation in CV apparent at low species richness suggested that other mechanisms besides species richness and evenness affected optical diversity. One possible explanation is the effects of species identity, in which individual species exert seemingly idiosyncratic effects on the relationship between optical diversity and vegetation diversity. To further explore this possibility, we considered the effects of species composition on CV. With the image-derived measurements, we

Table 4
Results of non-parametric multivariate analysis of variance (NPMANOVA), comparing among- and within-species spectral variation using Euclidean distance and overall accuracy and Kappa statistic of the PLS-DA classification.

Spectral region	Bands	NPMANOVA	PLSDA	
		F ratios	Overall accuracy	Kappa statistic
Leaf-level VIS-NIR (mean Ref[a])	601	–[b]	0.75	0.73
Leaf-level VIS-NIR (all samples)		113.02***	0.78	0.76
Leaf-level full spectra (mean Ref[a])	2001	–[b]	0.69	0.67
Leaf-level full spectra (all samples)		188.89***	0.80	0.77
Image-derived VIS-NIR (mean Ref[a])	762	–[b]	1	1
Image-derived VIS-NIR (all samples)		694.94***	0.73	0.70

[a] Mean reflectance of each species was used to generate the simulation plots.
[b] NPMANOVA was not applied to the mean reflectance data because the within species variation equals 0 in this case.
*** Indicates $p < 0.01$. p values were calculated by permutation since the distributions of the *F*-ratios are not distributed like Fisher's *F*-ratio under the null hypothesis (Anderson, 2001).

noticed two distinct trends in the CV-Shannon's index relationship depending upon the CV range (low or high): at low (CV < 0.5) values, we noted a positive CV-Shannon's index relationship, while at high (CV > 0.5) values, this trend was reversed (Table 7 and Fig. 6). Further exploration revealed that a single species, *Petalostemum villosum*, which had the largest within-species variation among all the species that indicated as the largest mean distance from centroid in spectral space (Fig. 3), was largely responsible for this effect. The decreasing CV-Shannon's index relationship indicated that a high percentage of species with large within-species variation (e.g. *Petalostemum villosum*) can lead to an anomalously high CV values within a plot. In this case, an increase in plot-level species diversity decreased the CV. This result revealed that besides species richness and evenness, species identity and spectral properties of specific species affect CV values and can confound the CV-biodiversity relationship.

3.4. Species-based optical diversity (PLS-DA classification)

When all spectra were included, higher classification accuracy and Kappa statistic values were achieved with leaf-level measurements than with image-derived measurements (Table 4). This was presumably a consequence of the image-derived spectra capturing more within-species variation than leaf-level spectra and thus overestimating the plot-level vegetation diversity. Most classification errors occurred among graminoid species (*Poa pratensis, Andropogon gerardi* and *Panicum virgatum*). For the leaf-level reflectance, using full range spectra increased the classification accuracy (Table 4), indicating that including information in the SWIR wavelengths increased the species separability.

The effect of using the mean reflectance vs. all spectra on biodiversity prediction accuracy changed between leaf-level and image-derived data. For leaf-level data, when the mean reflectance of each species was used instead of all individual spectra to test the PLSDA classifier, the classification accuracy declined from 0.78 to 0.75 using VIS-NIR wavelengths or from 0.80 to 0.69 using full-range spectra. By contrast, for image-derived data, the overall classification accuracy was actually highest (16/16) when using mean spectra, and declined to 0.73 when using all spectra (Table 4 and Fig. 7). When using mean reflectance spectra, species richness, Shannon's index and Simpson's index were underestimated by spectral species metrics using leaf-level data (Fig. 7 a, b, c). When using all reflectance spectra, vegetation diversity

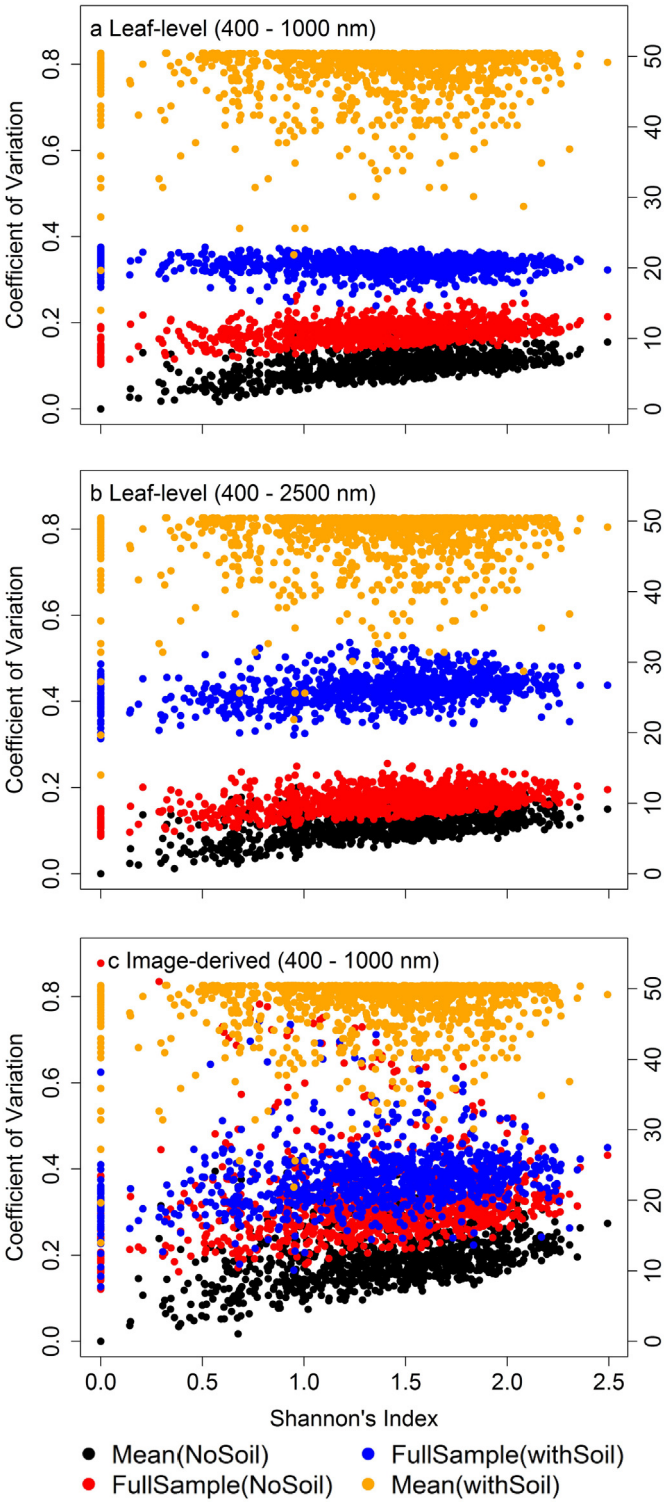

Fig. 4. Coefficient of variation (CV)-Shannon's index relationships from simulated plots using (a) leaf-level VIS-NIR spectra, (b) leaf-level full range, and (c) image-derived spectra. The CV calculated with soil spectra were plotted on the right Y-axis. The CV-biodiversity relationships were summarized in Table 5.

metrics were generally overestimated by spectral species metrics for both leaf-level and image-derived reflectance (Fig. 7d, e, f). This indicated that the spectral sampling method influenced the spectral separability in complex and seemingly contradictory ways that had significant implications for biodiversity estimation.

Table 5
Slopes and coefficient of determination (R^2) of regressions between coefficient of variation (CV) and vegetation diversity metrics (species richness (*S*), Shannon's index (*H′*), Simpson's index (*D*), and evenness (*J′*)) for different sampling methods and spectral ranges using simulated plots. Significance codes: NS, $0.05 < p$, *, $0.01 < p < 0.05$, **, $0.001 < p < 0.01$ and ***, $p < 0.001$.

	Mean reflectance (no soil)			Full sample (no soil)			Full sample (with soil)		
	Leaf clip-derived (VIS-NIR)	Leaf clip-derived (full range)	Image-derived (VIS-NIR)	Leaf clip-derived (VIS-NIR)	Leaf clip-derived (full range)	Image-derived (VIS-NIR)	Leaf clip-derived (VIS-NIR)	Leaf clip-derived (full range)	Image-derived (VIS-NIR)
S	0.0041 (0.27***)	0.0044 (0.25***)	0.0067 (0.18***)	0.002 (0.11***)	0.0023 (0.14***)	0.003 (0.01***)	−0.001 (0.06***)	0.0039 (0.25***)	0.006 (0.18***)
H′	0.031 (0.52***)	0.055 (0.51***)	0.082 (0.37***)	0.022 (0.23***)	0.029 (0.30***)	0.03 (0.03***)	NS	0.025 (0.15***)	0.038 (0.09***)
D	0.05 (0.51***)	0.016 (0.31***)	0.024 (0.22***)	0.007 (0.16***)	0.0094 (0.21***)	0.01 (0.02***)	NS	0.0057 (0.05***)	0.007 (0.02***)
J′	0.11 (0.37***)	0.12 (0.37***)	0.19 (0.32***)	0.05 (0.18***)	0.064 (0.22***)	0.1 (0.04***)	0.009 (0.01**)	NS	NS

4. Discussion

Vegetation canopy reflectance is influenced both by leaf traits and canopy structure (Ollinger, 2011), and it has been debated whether the estimation of some leaf level traits (e.g., leaf nitrogen content) could be confounded by canopy structure when retrieved from canopy level reflectance (Knyazikhin et al., 2013; Townsend et al., 2013). In this study, the different results with leaf-level vs. image-derived spectra have implications for studies that "scale up" from leaf to canopy or stand-scale to approximate canopy optical properties and estimate diversity. While leaf-level spectra emphasize differences in biochemical and structural traits of leaves, image-derived spectra also integrate effects of canopy structure and multiple scattering under natural illumination from multiple leaves and plants. When mean species spectra are used as a way of upscaling from leaf to canopy reflectance, leaf trait values are aggregated, eliminating the variation within species or the variation caused by canopy structure. Our unique tram dataset allowed us to explore the optical diversity-vegetation diversity relationship based on spectra that covered larger and presumably more realistic variations than leaf-level measurements alone, indicating that spectral variability of the canopy can both confound and enhance biodiversity assessments, depending upon the particular circumstance. It is also worth noting that for some species with tiny leaves, the leaves may not have filled the entire FOV of the leaf clip, leading to darker values than expected. Methods like brightness normalization (Feilhauer et al., 2010), although not used here, might be helpful in such cases.

4.1. Optical diversity: CV vs. spectral species

Diversity-indices based on information content have been used before to estimate biodiversity from satellite images (Rocchini, 2007; Rocchini et al., 2004), and this study introduced a methodology for examining this approach at much finer spatial scales. In keeping with previous studies, the CV reflects a combination of species richness and evenness, and is not always a good indicator for species richness alone (Wang et al., 2016a; Wang et al., 2018). For example, when species richness increases but evenness is low because a small number of species dominate the plot, the plot-level CV remains low. Instead, CV seems to best capture the combined effects of species richness and evenness, as measured by Shannon's and Simpson's indices.

When using spectral species (optical types), the accuracy of biodiversity estimation varied with the spectral training sample (leaf-level vs. image-derived) and the accuracy of the classification method. In this study, the larger variability of image-derived reflectance spectra incorporating leaf properties and canopy architecture with complex illumination and multiple scattering properties led to lower classification accuracy than when leaf-level reflectance was used. These results indicate that leaf traits and canopy traits can have independent and contrasting influence on optical diversity signals.

4.2. Species composition effects

Species identity substantially affected both categories of optical diversity indices: information content (CV) and species based (PLS-DA) metrics. This study illustrated two different plot-level diversity and composition scenarios that can generate high plot-level CV values: 1) high species richness and evenness, which have been described in previous spectral diversity studies (Rocchini et al., 2010; Wang et al., 2018); and 2) low species richness with large within-species spectral variability. In the second case, the CV of a high diversity plot simulated using image-derived reflectance was exceeded by the CV of a low diversity plot dominated by a species with large intraspecific spectral variability, *P. villosum* (Fig. 6). The large intra-specific variability of this species is possibly related to spatial variation resulting from the distribution of its tiny leaflets (each about 0.635 cm long) arranged in a dense and multi-layered pattern along the leaf rachises and plant stems. This species happened to be in flower during our measurements, which caused stem elongation and the emergence of bright purple flowers, presumably contributing to this variability in optical patterns at a fine scale. Canopy structure effects, along with the characteristics of other plant organs such as inflorescences and fruits, can lead to substantial illumination and scattering differences in image-derived reflectance but not in leaf-level measurements. Our study clearly demonstrated that both leaf traits and canopy structure influence optical diversity. Although the seemingly arbitrary threshold (CV = 0.5) we used in this study to split the data influenced by this single species may not hold for a different dataset, in this case, our results demonstrate that the presence or absence of certain species (*P. villosum* in this case, Fig. 6) can influence optical diversity and alter the optical diversity-vegetation diversity relationship. Apparently, single species can suddenly have disproportionate impacts on its optical properties, e.g., during flowering. It is worth noting that *P. villosum* was the only species in our study that had a much larger within-species variation than the other species (Figs. 3 and S2 in Supplemental section). In natural ecosystems or at other time periods, however, other species could possibly have large within-species variation in their optical signals caused by leaf traits, flowering, or variable canopy structure at particularly growth stages, possibly confounding the use of optical diversity to assess biodiversity, particularly when species-level information is not available.

4.3. Soil and litter background effects

The scattering and reflectance properties of non-vegetated background (e.g., soil and litter) affect canopy reflectance (Huete, 1988; van Leeuwen and Huete, 1996), and intermediate background cover (~50%) can have the greatest influence on overall vegetation canopy reflectance and vegetation indices as mixed pixels (Huete, 1988). At fine scales, our study indicated that the effects of background on detecting biodiversity through optical diversity varied with the selected

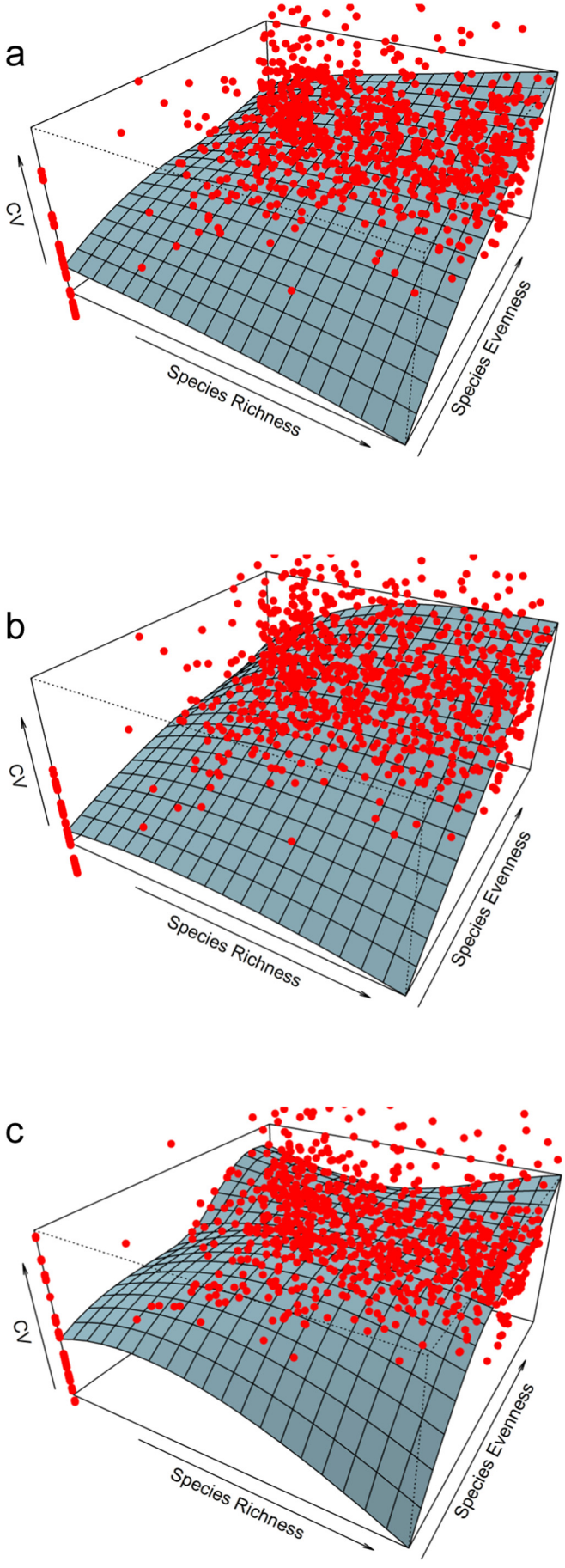

Fig. 5. Plot-level CV calculated using the full set of plant reflectance spectra as a function of species richness and evenness (soil spectra were not included). Species richness started from 1. The 3D surface was fitted with local polynomial regression. The CV was calculated using (a) leaf-level VIS-NIR (400–1000 nm), (b) leaf-level full spectral range (400–2500 nm), and (c) image-derived spectra. The ANOVA results of the CV-richness and CV-evenness relationships were summarized in Table 6.

Table 6
ANOVA results of CV-richness and CV-evenness relationships. Significant codes: NS, $0.05 < p$, *, $0.01 < p < 0.05$, **, $0.001 < p < 0.01$ and ***, $p < 0.001$.

Sampling method	Diversity metric	Mean sum of squares	*F* value
Leaf-level VIS-NIR mean reflectance	Richness	0.372	598.453***
	Evenness	0.389	626.353***
	Richness:Evenness	0.00091	1.464^{NS}
Leaf-level VIS-NIR full sample	Richness	0.0680	146.708***
	Evenness	0.0833	179.720***
	Richness:Evenness	0.000371	0.800^{NS}
Leaf-level full spec mean reflectance	Richness	0.435	531.219***
	Evenness	0.48	585.919***
	Richness:Evenness	0.00042	0.514^{NS}
Leaf-level full spec full sample	Richness	0.114	198.089***
	Evenness	0.145	250.608***
	Richness:Evenness	0.0018	3.1163^{NS}
Image-derived mean reflectance	Richness	0.976	323.54***
	Evenness	1.365	452.47***
	Richness:Evenness	0.0405	13.44***
Image-derived full sample	Richness	0.143	13.529***
	Evenness	0.376	35.501***
	Richness:Evenness	0.0881	8.319**

approach. Species-based (PLS-DA) spectral diversity metrics were less sensitive to soil background than the information content-based (CV) metrics because different backgrounds, which are often spectrally unique, can be accurately classified given high spatial resolution (Roth et al., 2015). It is possible to exclude soil pixels at fine scales, but it is less practical when scaling up because pixels at coarse scales are often mixtures of plants and soil. Results from another study revealed that excluding or correcting for soil effects improved the relationship between optical diversity and vegetation diversity (Gholizadeh et al., 2018). Clearly, the optical properties of different backgrounds, such as soil and litter, can confound optical diversity metrics (Fig. 4).

4.4. Choice of optical diversity metric

We suggest that there is likely no "one-size-fits-all" optical diversity metric that works universally to estimate vegetation diversity. It appears that the performance of optical diversity metrics should be based on the properties of the available data, the particular goals of the study, and the scale of the sampling (Wang et al., 2018). In general, both within- and among- species variation in reflectance properties influence the ability of optical diversity indices to assess biodiversity. In accordance with Roth et al., 2015, conditions having larger within-species variation than among-species variation complicates accurate detection of biodiversity using CV (Table 5) and PLS-DA classification (Fig. 7).

Species-based (PLS-DA) metrics combined with a priori species information might work better than information content-methods (CV) when each species has a dense distribution in spectral space and the spectral distances between species is large enough to distinguish one species from another. It has been reported that classification methods can be applied to high-resolution imaging spectrometry to determine optical diversity and thus biodiversity (Féret and Asner, 2014). However, species-based methods (PLS-DA) fail when it is impossible to find spectral endmembers or pure pixels, such that images consist of mixed pixels, or when species are too similar to be spectrally separated. The

Table 7
Statistical relationships between the CV and Shannon's index using different sampling methods and spectral ranges (soil spectra were not included).

Sampling method	Regression parameters			
	Intercept	Slope	R^2	*p* value
Leaf-level VIS-NIR	0.149	0.022	0.23	2.2e-16
Leaf-level full range	0.129	0.029	0.30	2.2e-16
Image-derived (CV < 0.5)	0.246	0.047	0.15	2.2e-16
Image-derived (CV > 0.5)	0.837	−0.15	0.58	1.9e-12

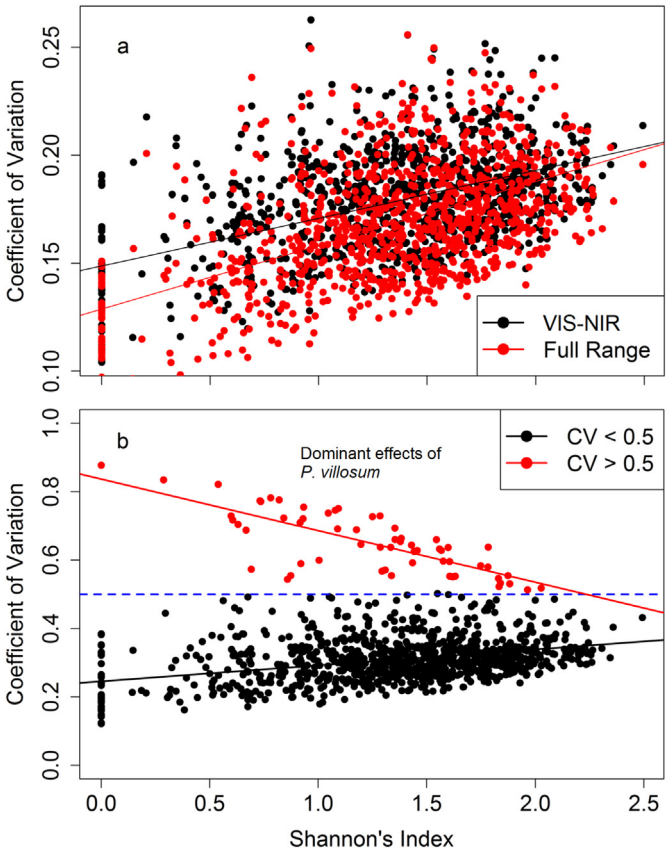

Fig. 6. Relationship between the coefficient of variation (CV) and Shannon's index from the simulated plots using (a) the full datasets of leaf-level reflectance, and (b) image-derived reflectance. Soil reflectance was not included. Regression parameters were shown in Table 7. Red line in panel b illustrates the dominant effect of a single species (*Petalostemum villosum*). (For interpretation of the references to color in this figure legend, the reader is referred to the web version of this article.)

accuracy decreases when scaling up to large pixel sizes due to information loss (Clark et al., 2005). Thus, the choice and success of a particular optical diversity metric is likely scale-dependent (Wang et al., 2018).

4.5. Unresolved questions

Timing and duration of sampling can have a profound influence on biodiversity estimates, making it difficult to detect community diversity from measurements at a single time point (Magurran, 2007). Including information about vegetation phenology increases the spectral separability of species and should improve predictions of vegetation diversity (Clark and Roberts, 2012). Therefore, including optical measurements across the whole growing season would likely increase classification accuracy for species that vary phenologically and whose optical properties are affected by leaf age, leaf drop, flowering and fruiting (Jiménez and Díaz-Delgado, 2015). For example, leaf aging and senescence can cause high variation within individual tree canopies on par with the variation detected among different individuals of the same species or of that detected between species in leaf morphological, biochemical and spectral traits of tropical tree species (Chavana-Bryant et al., 2017). Studies have also shown that the biodiversity-productivity relationship can vary across the growing season (Wang et al., 2016b).

This study focused on the optical properties of prairie plants during peak growing season. We would expect different optical diversity-vegetation diversity relationships for contrasting biomes and communities, e.g. prairie (with small plant sizes) versus forests (where tree crown size is typically several meters in diameter). Additionally, we would expect that inclusion of phenological variation in spectral properties to alter the results, so multitemporal studies are clearly needed. Many studies have shown that it is possible to classify tree species using airborne hyperspectral remote sensing (Asner et al., 2008; Paz-Kagan et al., 2017) or airborne LiDAR (Clawges et al., 2008; Seidel et al., 2013). However, there are few studies that investigate the optical diversity of forest ecosystems at fine scales (e.g., pixel size of 10 cm or smaller). Our recent work, while limited to a prairie system, clearly demonstrates that consideration of spatial scale is important when assessing biodiversity from remote sensing (Wang et al., 2018). Data from contrasting ecosystems and vegetation types, including complex landscapes (e.g. prairie and forest combined), should be included in future studies, with attention to the consequences of leaf traits and canopy structure, spatial scale, and landscape structure on the optical-vegetation diversity relationship. If conducted at multiple scales, such studies would help reveal the length scales (pixel sizes or spatial lags) at which optical diversity can best detect various metrics of biodiversity as defined by biologists. Such studies are essential if we are to develop reliable operational approaches for remote sensing of biodiversity.

5. Conclusions

This study used leaf-level and image-derived reflectance spectra and a simulation approach to investigate how species richness, evenness and composition affect the detectability of vegetation α diversity with optical diversity. The modeling framework allowed us to isolate factors contributing to the overall optical signal, such as leaf traits, canopy structure, and background effects in a way that is not possible from a single set of empirical measurements alone. We tested two metrics of optical diversity, one based on information content (CV), and the other based on spectral species (PLS-DA). We confirmed that optical diversity was affected by both species richness and evenness. Species identity substantially affected both categories of optical diversity metrics (information content-based and species-based), especially for species with high intra-specific variation. Soil background effects varied with diversity metrics: information content-based metrics were sensitive to the background, while background had limited effects on species-based metrics. Our results demonstrate that sampling method and choice of optical diversity indices can influence the ability to assess vegetation diversity using remote sensing, and the best choice of optical diversity metric will depend upon the particular study. Compared to leaf clip-derived data, image-derived data have the ability to capture larger within-species variability caused by differences in plant geometry and illumination. As a consequence, image-derived data might provide a more realistic way for assessing biodiversity using remote sensing techniques than leaf-level data. The modeling approach used here can help provide insights into the development of robust operational methods for remote sensing of biodiversity.

Acknowledgements

We thank staff at the Cedar Creek Ecosystem Science Reserve, particularly Troy Mielke and Kally Worm. Ian Carriere and Brett

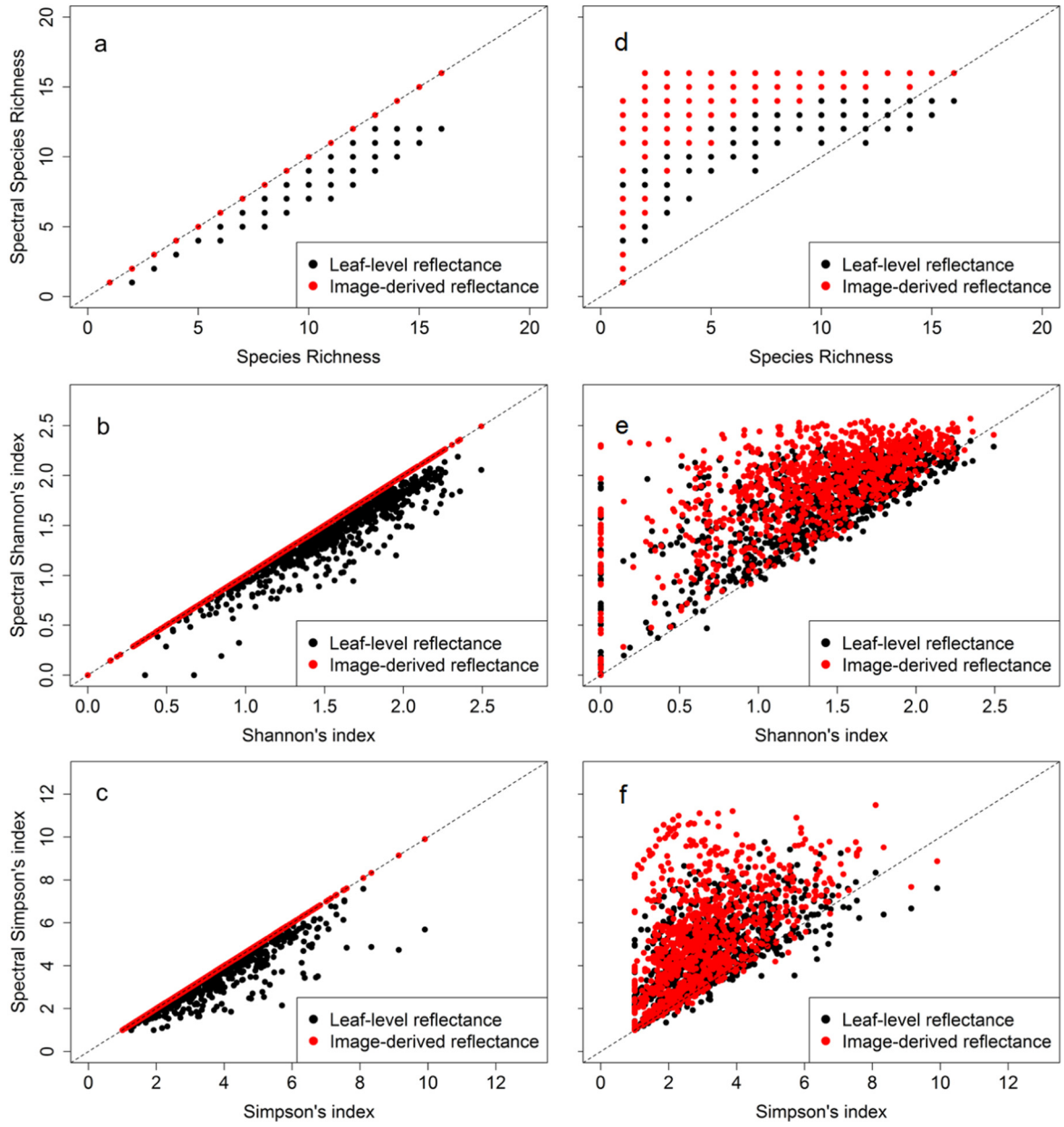

Fig. 7. Relationships between spectral species richness (a and d), spectral Shannon's index (b and e), and spectral Simpson's index (c and f), based on the PLS-DA classification for mean reflectance (a–c) and full sample reflectance (d–f) and vegetation diversity metrics for all simulated plots. The dotted line in each panel represented the 1:1 line.

Fredericksen helped with leaf reflectance measurements and Ben Paulat helped with obtaining hyperspectral images. This study was supported by NASA and NSF grants (DEB-1342872 and 1342823) and a NSF-LTER grant (DEB-1234162) to J. Cavender-Bares, and by iCORE/AITF (G224150012 & 200700172), NSERC (RGPIN-2015-05129), and CFI (26793) grants to J. Gamon, and a China Scholarship Council fellowship to R. Wang.

Appendix A. Supplementary data

Supplementary data to this article can be found online at https://doi.org/10.1016/j.rse.2018.04.010.

References

Anderson, M.J., 2001. A new method for non parametric multivariate analysis of variance. Austral Ecol. 26 (2001), 32–46. http://dx.doi.org/10.1111/j.1442-9993.2001.01070.pp.x.

Asner, G.P., 1998. Biophysical and biochemical sources of variability in canopy reflectance. Remote Sens. Environ. 64, 234–253.

Asner, G.P., Martin, R.E., 2009. Airborne spectranomics: mapping canopy chemical and taxonomic diversity in tropical forests. Front. Ecol. Environ. 7 (5), 269–276. http://dx.doi.org/10.1890/070152.

Asner, G.P., Jones, M.O., Martin, R.E., Knapp, D.E., Hughes, R.F., 2008. Remote sensing of native and invasive species in Hawaiian forests. Remote Sens. Environ. 112 (5), 1912–1926. http://dx.doi.org/10.1016/j.rse.2007.02.043.

Carlson, K.M., Asner, G.P., Hughes, R.F., Ostertag, R., Martin, R.E., 2007. Hyperspectral remote sensing of canopy biodiversity in Hawaiian lowland rainforests. Ecosystems 10 (4), 536–549. http://dx.doi.org/10.1007/s10021-007-9041-z.

Chavana-Bryant, C., Malhi, Y., Wu, J., Asner, G.P., Anastasiou, A., Enquist, B.J., ... Gerard, F.F., 2017. Leaf aging of Amazonian canopy trees as revealed by spectral and physiochemical measurements. New Phytol 214 (3), 1049–1063. http://dx.doi.org/10.1111/nph.13853.

Chung, D., Keles, S., 2010. Sparse partial least squares classification for high dimensional data. Stat. Appl. Genet. Mol. Biol. 9 (1), 17. http://dx.doi.org/10.2202/1544-6115.1492.

Clark, M.L., Roberts, D.A., 2012. Species-level differences in hyperspectral metrics among tropical rainforest trees as determined by a tree-based classifier. Remote Sens. 4 (12), 1820–1855. http://dx.doi.org/10.3390/rs4061820.

Clark, M.L., Roberts, D.A., Clark, D.B., 2005. Hyperspectral discrimination of tropical rain forest tree species at leaf to crown scales. Remote Sens. Environ. 96, 375–398. http://dx.doi.org/10.1016/j.rse.2005.03.009.

Clawges, R., Vierling, K., Vierling, L., Rowell, E., 2008. The use of airborne lidar to assess avian species diversity, density, and occurrence in a pine/aspen forest. Remote Sens. Environ. 112 (5), 2064–2073. http://dx.doi.org/10.1016/j.rse.2007.08.023.

Feilhauer, H., Asner, G.P., Martin, R.E., Schmidtlein, S., 2010. Brightness-normalized Partial Least Squares Regression for hyperspectral data. J. Quant. Spectrosc. Radiat. Transf. 111 (12 − 13), 1947–1957. http://dx.doi.org/10.1016/j.jqsrt.2010.03.007.

Féret, J.-B., Asner, G.P., 2014. Mapping tropical forest canopy diversity using high-fidelity imaging spectroscopy. Ecol. Appl. 24 (6), 1289–1296. http://dx.doi.org/10.1890/13-1824.1.

Gamon, J.A., Cheng, Y., Claudio, H., MacKinney, L., Sims, D.A., 2006. A mobile tram system for systematic sampling of ecosystem optical properties. Remote Sens. Environ. 103, 246–254. http://dx.doi.org/10.1016/j.rse.2006.04.006.

Gholizadeh, H., Gamon, J.A., Zygielbaum, A.I., Wang, R., Schweiger, A.K., Cavender-Bares, J., 2018. Remote sensing of biodiversity: soil correction and data dimension reduction methods improve assessment of α-diversity (species richness) in prairie ecosystems. Remote Sens. Environ. 206 (November 2017), 240–253. http://dx.doi.org/10.1016/j.rse.2017.12.014.

Gould, W., 2000. Remote sensing of vegetation, plant species richness, and regional biodiversity hotspots. Ecol. Appl. 10 (6), 1861–1870.

Huete, A.R., 1988. A soil-adjusted vegetation index (SAVI). Remote Sens. Environ. 25 (3), 295–309. http://dx.doi.org/10.1016/0034-4257(88)90106-X.

Jiménez, M., Díaz-Delgado, R., 2015. Towards a standard plant species spectral library protocol for vegetation mapping: a case study in the Shrubland of Doñana National Park. ISPRS Int. J. Geo-Inf. 4 (4), 2472–2495. http://dx.doi.org/10.3390/ijgi4042472.

Knyazikhin, Y., Schull, M.A., Stenberg, P., Mõttus, M., Rautiainen, M., Yang, Y., ... Myneni, R.B., 2013. Hyperspectral remote sensing of foliar nitrogen content. Proc. Natl. Acad. Sci. U. S. A. 110 (3), E185–192. http://dx.doi.org/10.1073/pnas.1210196109.

Kuhn, M., 2008. Building predictive models in R using the caret package. J. Stat. Softw. 28 (5), 1–26. http://dx.doi.org/10.1053/j.sodo.2009.03.002.

van Leeuwen, W.J.D., Huete, A.R., 1996. Effects of standing litter on the biophysical interpretation of plant canopies with spectral indices. Remote Sens. Environ. 55 (2), 123–138. http://dx.doi.org/10.1016/0034-4257(95)00198-0.

Magurran, A.E., 2007. Species abundance distributions over time. Ecol. Lett. 10 (5), 347–354. http://dx.doi.org/10.1111/j.1461-0248.2007.01024.x.

Nguyen, D.V., Rocke, D.M., 2002. Multi-class cancer classification via partial least squares with gene expression profiles. Bioinformatics 18 (9), 1216–1226. http://dx.doi.org/10.1093/bioinformatics/18.9.1216.

Oldeland, J., Wesuls, D., Rocchini, D., Schmidt, M., Jürgens, N., 2010. Does using species abundance data improve estimates of species diversity from remotely sensed spectral heterogeneity? Ecol. Indic. 10, 390–396. http://dx.doi.org/10.1016/j.ecolind.2009.07.012.

Ollinger, S.V., 2011. Sources of variability in canopy reflectance and the convergent properties of plants. New Phytol. 189, 375–394. http://dx.doi.org/10.1111/j.1469-8137.2010.03536.x.

Palmer, M.W., Earls, P.G., Hoagland, B.W., White, P.S., Wohlgemuth, T., 2002. Quantitative tools for perfecting species lists. Environmetrics 13, 121–137. http://dx.doi.org/10.1002/env.516.

Paz-Kagan, T., Caras, T., Herrmann, I., Shachak, M., Karnieli, A., 2017. Multiscale mapping of species diversity under changed land use using imaging spectroscopy. Ecol. Appl. 27 (5), 1466–1484. http://dx.doi.org/10.1002/eap.1540.

Peerbhay, K.Y., Mutanga, O., Ismail, R., 2013. Commercial tree species discrimination using airborne AISA Eagle hyperspectral imagery and partial least squares discriminant analysis (PLS-DA) in KwaZulu-Natal, South Africa. ISPRS J. Photogramm. Remote Sens. 79, 19–28. http://dx.doi.org/10.1016/j.isprsjprs.2013.01.013.

Pielou, E.C., 1966. The measurement of diversity in different types of biological collections. J. Theor. Biol. 13, 131–144. http://dx.doi.org/10.1016/0022-5193(67)90048-3.

Reich, P.B., Tilman, D., Isbell, F., Mueller, K., Hobbie, S.E., Flynn, D.F.B., Eisenhauer, N., 2012. Impacts of biodiversity loss escalate through time as redundancy fades. Science 336 (6081), 589–592. http://dx.doi.org/10.1126/science.1217909.

Roberts, D.A., Ustin, S.L., Ogunjemiyo, S., Greenberg, J., Dobrowski, S.Z., Chen, J., Hinckley, T.M., 2004. Spectral and structural measures of northwest forest vegetation at leaf to landscape scales. Ecosystems 7 (5), 545–562. http://dx.doi.org/10.1007/s10021-004-0144-5.

Rocchini, D., 2007. Effects of spatial and spectral resolution in estimating ecosystem α-diversity by satellite imagery. Remote Sens. Environ. 111, 423–434. http://dx.doi.org/10.1016/j.rse.2007.03.018.

Rocchini, D., Chiarucci, A., Loiselle, S.A., 2004. Testing the spectral variation hypothesis by using satellite multispectral images. Acta Oecol. 26, 117–120. http://dx.doi.org/10.1016/j.actao.2004.03.008.

Rocchini, D., Balkenhol, N., Carter, G.A., Foody, G.M., Gillespie, T.W., He, K.S., ... Neteler, M., 2010. Remotely sensed spectral heterogeneity as a proxy of species diversity: recent advances and open challenges. Eco. Inform. 5, 318–329. http://dx.doi.org/10.1016/j.ecoinf.2010.06.001.

Roth, K.L., Roberts, D.A., Dennison, P.E., Alonzo, M., Peterson, S.H., Beland, M., 2015. Differentiating plant species within and across diverse ecosystems with imaging spectroscopy. Remote Sens. Environ. 167, 135–151. http://dx.doi.org/10.1016/j.rse.2015.05.007.

Schäfer, E., Heiskanen, J., Heikinheimo, V., Pellikka, P., 2016. Mapping tree species diversity of a tropical montane forest by unsupervised clustering of airborne imaging spectroscopy data. Ecol. Indic. 64, 49–58. http://dx.doi.org/10.1016/j.ecolind.2015.12.026.

Seidel, D., Leuschner, C., Scherber, C., Beyer, F., Wommelsdorf, T., Cashman, M.J., Fehrmann, L., 2013. The relationship between tree species richness, canopy space exploration and productivity in a temperate broad-leaf mixed forest. For. Ecol. Manag. 310, 366–374.

Shannon, C.E., 1948. A mathematical theory of communication. Bell Syst. Tech. J. 27 (379–423), 623–656. http://dx.doi.org/10.1145/584091.584093.

Simpson, E.H., 1949. Measurement of diversity. Nature 163, 688. http://dx.doi.org/10.1038/163688a0.

Thompson, D.R., Boardman, J.W., Eastwood, M.L., Green, R.O., 2017. A large airborne survey of Earth's visible-infrared spectral dimensionality. Opt. Express 25 (8), 9186. http://dx.doi.org/10.1364/OE.25.009186.

Tilman, D., 1997. The influence of functional diversity and composition on ecosystem processes. Science 277, 1300–1302. http://dx.doi.org/10.1126/science.277.5330.1300.

Tilman, D., Reich, P.B., Knops, J., Wedin, D., Mielke, T., Lehman, C., 2001. Diversity and productivity in a long-term grassland experiment. Science 294 (5543), 843–845. http://dx.doi.org/10.1126/science.1060391.

Townsend, P.A., Serbin, S.P., Kruger, E.L., Gamon, J.A., 2013. Disentangling the contribution of biological and physical properties of leaves and canopies in imaging spectroscopy data. Proc. Natl. Acad. Sci. U. S. A. 110 (12), E1074. http://dx.doi.org/10.1073/pnas.1300952110.

Ustin, S.L., Gamon, J.A., 2010. Remote sensing of plant functional types. New Phytol. 186, 795–816.

Ustin, S.L., Gitelson, A.a., Jacquemoud, S., Schaepman, M., Asner, G.P., Gamon, J.A., Zarco-Tejada, P.J., 2009. Retrieval of foliar information about plant pigment systems from high resolution spectroscopy. Remote Sens. Environ. 113, S67–S77. http://dx.doi.org/10.1016/j.rse.2008.10.019.

Wang, R., Gamon, J.A., Emmerton, C.A., Li, H., Nestola, E., Pastorello, G.Z., Menzer, O., 2016a. Integrated analysis of productivity and biodiversity in a southern Alberta prairie. Remote Sens. 8 (3), 214.

Wang, R., Gamon, J.A., Montgomery, R.A., Townsend, P.A., Zygielbaum, A.I., Bitan, K., ... Cavender-Bares, J., 2016b. Seasonal variation in the NDVI–species richness relationship in a prairie grassland experiment (Cedar Creek). Remote Sens. 8 (2), 128. http://dx.doi.org/10.3390/rs8020128.

Wang, R., Gamon, J.A., Cavender-Bares, J., Townsend, P.A., Zygielbaum, A.I., 2018. The spatial sensitivity of the spectral diversity-biodiversity relationship: an experimental test in a prairie grassland. Ecol. Appl. 28 (2), 541–556. http://dx.doi.org/10.1002/eap.1669.

Williams, C.B., 1964. Patterns in the Balance of Nature and Related Problems in Quantitative Ecology. Academic Press, London.